Hindawi
Advances in Materials Science and Engineering
Volume 2023, Article ID 5585132, 13 pages
https://doi.org/10.1155/2023/5585132

Research Article

Synthesis and Empirical Analysis of the Thermophysical Characteristics of GO-Ag Aqueous Hybrid Nanofluid Using Environmentally Friendly Reducing and Stabilizing Agents

M. Armstrong,[1] **M. Sivasubramanian**,[1] **N. Selvapalam**,[2] **R. Pavitra**,[2] **P. Rajesh Kanna**,[3] **and Haiter Lenin**[4]

[1]*School of Mechanical, Aero, Auto and Civil Engineering, Kalasalingam Academy of Research and Education, Virudhunagar, Tamil Nadu, India*
[2]*School of Advanced Sciences, Kalasalingam Academy of Research and Education, Virudhunagar, Tamil Nadu, India*
[3]*CO_2 Research and Green Technologies Centre, Vellore Institute of Technology, Vellore, Tamil Nadu, India*
[4]*Department of Mechanical Engineering, WOLLO University, Kombolcha Institute of Technology, Post Box No: 208, Kombolcha, Ethiopia*

Correspondence should be addressed to M. Armstrong; mecharmstrong@gmail.com and Haiter Lenin; haiter@kiot.edu.et

Received 20 January 2023; Revised 4 September 2023; Accepted 13 September 2023; Published 4 October 2023

Academic Editor: Ajay Kumar Mishra

The remarkable potential of the carbon allotrope graphene and its derivatives in developing hybrid nanofluids has sparked considerable interest among researchers. These carbon nanoparticles offer excellent opportunities to blend with various metal or metal oxide nanoparticle binders to improve their material properties. This study focuses on investigating the synthesis, characterization, and thermophysical properties of silver- (Ag-) infused GO aqueous hybrid nanofluids with various weight percentages (0.025, 0.05, and 0.1 wt.%) using environmentally friendly reducing and stabilizing agents. Characterization of the hybrid nanofluids was performed using XRD, SEM, EDX, a UV-visible spectrometer, a particle size analyzer, and FTIR techniques. The thermal conductivity and viscosity of the GO-Ag hybrid nanofluids were experimentally determined in the temperature range of 293 K–333 K. Notably, the results indicated that the nanofluids with a concentration of 0.1 wt.% exhibited the most significant enhancement in thermal conductivity, with improvements of 15.22% at 293 K and 31.19% at 333 K compared to the base fluid. A mathematical model was developed based on the thermal conductivity experimental results using the response surface methodology (RSM). Overall, the results suggest that the silver nanoparticles-decorated aqueous graphene oxide hybrid nanofluid has promising potential as an innovative heat transfer fluid in various heat transfer applications.

1. Introduction

The use of graphene-based nanoparticles in both solid metal structures and liquids has created opportunities for various applications such as thermal power generation, clean and renewable energy, heat transfer, electronic cooling, and bioenergy. This is because graphene nanoparticles have better chemical, mechanical, electrical, and thermophysical properties [1–5]. However, there are some challenges associated with graphene nanoparticles, such as difficulties in bulk production and their hydrophobic nature, which leads to low stability with water. These issues led to the development of graphene oxide (GO) as one of the alternatives to graphene. These GO nanoparticles are simple to prepare on a large scale, are cost-effective, have high thermal conductivity, and are hydrophilic towards water molecules, making them an ideal candidate for thermal investigations [1, 6]. To this end, Hajjar et al. [7] studied the thermal conductivity of five different concentrated GO nanofluids (0.05 wt.%–0.25 wt.%) at operating temperatures ranging from 10°C to 40°C. The authors found that at 40°C and 0.25 wt.%, there was a maximum increase in thermal conductivity of 47.54%.

The authors also noted that the thermal conductivity of the GO nanofluid increased with temperature and nanoparticle concentration. In a similar vein, the research conducted by Mei et al. [8] delved into the thermal and rheological characteristics of GO nanofluids with low mass fractions ranging from 0.002% to 0.01% at temperatures between 25°C and 50°C. The authors discovered that at 0.01% and 50°C, the GO nanofluid displayed higher thermal conductivity than other low concentrations. The authors' observations mirrored those of Hajjar et al., and they further reported that an increase in temperature and nanoparticle concentration led to a decrease and increase in nanofluid viscosity, respectively. The literature discussed above indicates that GO nanofluids can substantially enhance the thermal conductivity of base fluids even at low concentrations. GO nanostructures possess multiple characteristics, including a higher surface-to-volume ratio, high charge carrier mobility, high thermal conductivity, tunable porosity and band gap, good catalytic properties as electron acceptors, high elasticity, longer stability duration, and many more, depending on the application requirements [9]. These multiple combinational characteristics make GO nanoparticles suitable for use as mono or hybrid nanoparticles. Several researchers have used GO nanoparticles as a core material and doped them with metal and metal oxide nanoparticles [10–14] to produce novel hybrid nanoparticles or nanofluids. The thermophysical, optical, chemical, and biological properties of the doped nanoparticles were enhanced through this process. For instance, Li et al. [15] prepared an ethylene glycol-based GO-Ag hybrid nanofluid and observed an increase in thermal conductivity of 22% at 45°C with a mass fraction of 0.3 wt.% in the temperature and mass fraction range of 20–45°C and 0.1, 0.2, and 0.3 wt.%, respectively. Later, the researcher Huminic et al. [16] conducted research on a GO-Si aqueous hybrid nanofluid and reported empirical and numerical findings on the nanofluid's viscosity impact at temperatures ranging from 20–50°C. They provided a detailed report indicating that the nanofluid's thermal performance would improve due to the reduction in viscosity at higher temperatures. Singh et al. [17] found a 30% improvement in the thermal conductivity of GO-CuO/DW nanofluids at 0.3 wt.% and 60°C. Taherialekouhi et al. [18] discussed the preparation of aqueous GO-Al_2O_3 hybrid nanofluid at 0.1, 0.25, 0.5, 0.75, and 1% volume fractions from 25–50°C and found 33.9% improvement in the thermal conductivity at 1% and 50°C. The authors also performed mathematical modelling for the experimental thermal conductivity ratio results, influencing the volume fraction and change in temperature of the hybrid nanofluid. El-Shafai et al. [19] investigated the thermal characteristics and ability of ternary GO@CuO/Al_2O_3 hybrid nanofluids in solar applications. The researchers observed a 22.56% improvement in thermal conductivity compared to the aqueous base fluid at 0.2 wt.% and 50°C. As a result, much research has been conducted on using GO as a core material for doping with metal oxides rather than metal nanoparticles and at higher concentrations instead of low concentrations.

This study focuses on the synthesis, characterization, and investigation of the stability and thermophysical characteristics of hybrid nanofluids containing Ag-decorated GO nanoparticles. The nanofluid is prepared with nanoparticle dispersions of less than 0.5 wt.% and at various weight percentages (0.025 wt.%, 0.05 wt.%, 0.1 wt.%) in doubled distilled water (DW). Furthermore, the response surface methodology (RSM) is employed to analyse the experimental thermal conductivity results. The RSM approach is crucial for performing precise regression analysis to forecast the mathematical model using experimental data. Previous studies have used RSM multivariate regression to evaluate the thermal characteristics of different nanofluids associated with input data such as temperatures and weight volume concentrations [20–22].

2. Materials and Procedures

2.1. Graphene Oxide (GO) Nanoparticles Fabrication. In this research, all chemicals purchased were of analytical grade and sourced from Sigma Aldrich, USA; Otto Chemie Private Ltd; Avra Synthesis Private Ltd; and Sisco Research Laboratories Pvt Ltd, India. The graphene oxide nanoparticles were synthesized using Hummer's modified approach [12, 23]. Initially, 3 grams of natural graphite flakes were combined with 3 grams of $NaNO_3$ in a purified 500 mL round-bottom flask. Then, 90 mL of concentrated H_2SO_4 was added with vigorous agitation at 0–5°C. After 3 to 4 hours, 12 g of solid $KMnO_4$ was slowly added in parts at temperatures below 15°C in an ice bath attributable to an exothermic reaction. The addition of chemicals was done at a slow pace. After 2 hours, 184 ml of distilled water was incorporated, and the compound was continuously stirred at room temperature for about two hours. The slurry was then refluxed at 98°C for 15 minutes, cooled to room temperature (RT), and agitated for two hours. The solution turned bright yellow after gently infusing 40 ml of H_2O_2 and was swirled for an hour with 400 ml of distilled water. The upper layer of water was subsequently extracted, followed by the addition of 10% HCl. The mixture was then subjected to centrifugation, and this process was repeated multiple times. The GO nanoparticles were washed with DW until the pH approached neutral, culminating in a gel-like material. The nanoparticles were dried at 60°C in a vacuum hot air oven and preserved in the dark.

2.2. GO-Ag Hybrid Nanoparticles Synthesis. Figure 1 presents a graphical representation of the synthesis process and molecular structure of GO-Ag hybrid nanoparticles. The GO-Ag nano-hybrids were prepared using presynthesized GO nano powder and Ag metal precursor derived from silver nitrate ($AgNO_3$), following established procedures [12, 24]. Silver nanoparticles (AgNPs) were obtained by reducing $AgNO_3$ in an aqueous solution with ascorbic acid as the reducing agent and trisodium citrate as the stabilizing agent to control the size and shape of the silver nanoparticles [25]. The typical process involved sonicating 1 g of GO in 100 ml of the aqueous solution for 2 hours. Subsequently,

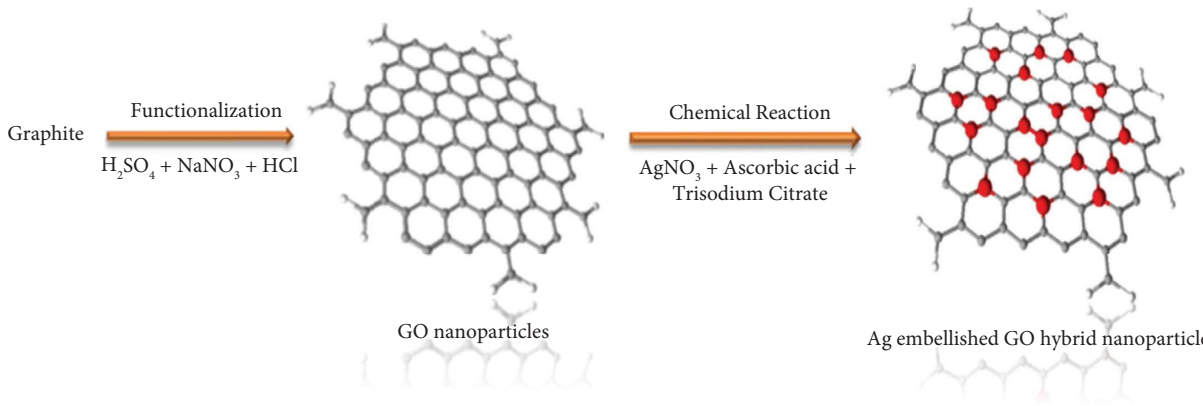

Figure 1: Graphical depiction of the process and molecular structure of GO-Ag hybrid nanoparticles.

6×10^{-2} M $AgNO_3$ dissolved in 100 ml of the aqueous solution, along with an aqueous trisodium citrate solution (1 ml, 10^{-3} M) and freshly prepared ascorbic acid (1 ml, 10^{-3} M), was gradually added to the $AgNO_3$ solution while continuously mixing for 1 hour at room temperature (RT). The resulting solution containing silver nanoparticles was added dropwise to the GO nano-solution while stirring at a constant speed of 90 rpm using a magnetic stirrer. The mixture was then left undisturbed for 48 hours at room temperature in the absence of light and without heating, resulting in the formation of GO-Ag-doped solutions. The GO-Ag solutions underwent centrifugation and were rinsed with DW and ethanol five times. Finally, they were cured at 50°C in a vacuum hot air oven to produce Ag-decorated hybrid nanoparticles.

2.3. GO-Ag Nanofluid Synthesis. A two-step approach was utilized to prepare the GO-Ag hybrid nanofluids from doubled distilled water and the synthesized hybrid nanoparticles of GO-Ag. After fixing the mass of the base fluid (m_{bf}) and the weight percentage of nanoparticles (φ), the mass of the synthesized hybrid nanoparticles was estimated using the following equation:

$$m_{np} = \frac{\varphi . m_{bf}}{1 - \varphi}. \quad (1)$$

The mass (m_{np}) of the synthesized GO-Ag nanohybrids was measured utilizing a high-precision digital balance (0.001 g). To obtain the various weight percentages (0.025%, 0.05%, and 0.1%) of the hybrid nanofluids, the respective known masses of the hybrid nanoparticles and the base fluid were mixed in an ultrasonic device for 30 minutes. Subsequently, constant stirring was carried out in a magnetic stirrer for one hour to achieve better dispersion of the hybrid nanofluids.

2.4. Morphological Characterization of GO-Ag Nanomaterials. Powder X-ray diffraction (XRD-D8 Advance ECO Bruker), scanning electron microscope (SEM, EVO 18, CARL ZEISS, Jena, Germany) at 30 kV, Fourier Transform Infra-Red Spectrophotometer (IR Tracer-100 Shimadzu), particle size analyzer (Horiba SZ-100Z), energy dispersive X-ray spectrometer (EDAX, Quantax 200 with X-Flash), and UV visible spectrometer (SL210, Elico, India) had been used to characterize the topologies of the synthesized GO-Ag nanohybrids.

2.5. Measurement of Thermophysical Properties. A viscometer (LVDVE, Brookfield Engineering Labs, USA) was used to test the viscosities of the nanofluids, which has a precision of ±1%. A KD2 Pro thermal property analyzer (Decagon Devices Inc., USA) employs a KS-1 sensor in a measurement range of 0.02–2 W/m. K and a precision of ±5%.

3. Findings and Critical Analysis

3.1. Findings of XRD. The X-ray diffraction pattern of the Ag deposition on the GO nanosheet is depicted in Figure 2, using the copper anode ($k_{\alpha 1} = 1.54060$). The diffractograms display steep peaks and broad patterns, indicating the presence of crystalline elements. The percentages of crystalline and amorphous phases confirm the deposition of Ag over GO at 36.95% and 63.05%, respectively. The diffracted peaks at Braggs angle $2\theta = 11.1^{\circ}$ and 16.94° confirm the presence of GO, while the peaks of Ag were observed at scattering angles of 38.1°, 44.3°, 64.5°, and 77.3° with h k l plane indices of (111), (200), (220), and (311). These peaks matched the space group Fm-3m with JCPDS Card no. 07-0783 [24], indicating the successful synthesis of the Ag-decorated GO hybrid nanoparticle.

3.2. Findings of FTIR. The investigation of the associations among all synthesized elements was conducted using the FTIR spectrum analysis. The transmittance proportion and wavenumbers of GO and GO-Ag hybrid nanoparticles were compared. Figure 3 shows that the broad spectral band at 3380.2 cm^{-1} and 1060.78 cm^{-1} corresponds to the O-H bending vibration of carboxylic acid and phenolic acid structural units, which indicates the presence of GO nanosheet [12]. The wavenumber 2360.71 cm^{-1} indicates the C-O bond, representing the bonding of crystalline elements.

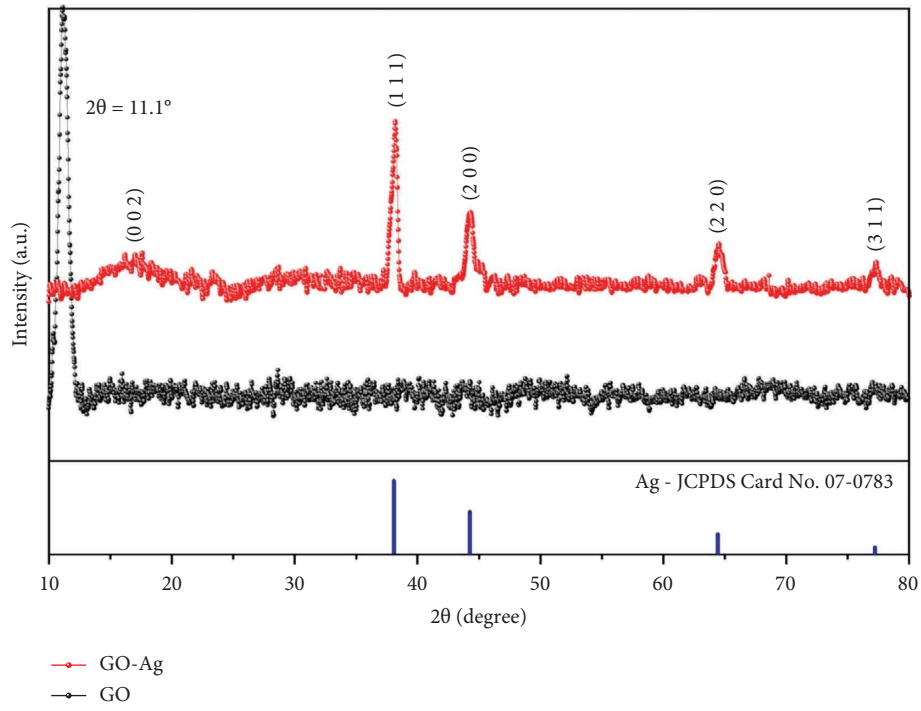

Figure 2: X-Ray diffractogram pattern of GO and GO-Ag hybrid nanoparticles.

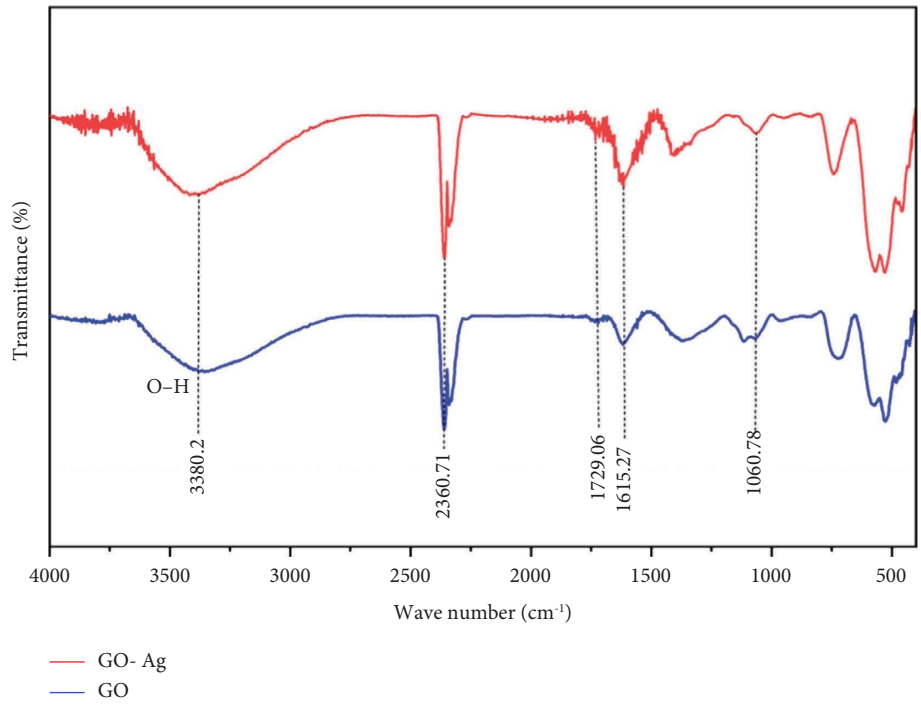

Figure 3: Results on FTIR spectra of GO and GO-Ag hybrid nanoparticles.

The functional bands at 1729.6 cm^{-1} and 1615.27 cm^{-1} are attributed to the asymmetric and symmetric carbonyl stretch vibrations of COOH groups (C=O), respectively. In the GO-Ag spectral bands, the peaks of the GO spectrum were reduced due to the doping of Ag nanoparticles over the GO layer.

The contact between the silver nanoparticles and the GO nanosheets' functional groups encompassing oxygen was stable by reversing the asymmetric and symmetric stretching processes. That is, the depth of the asymmetric –(COO) elongation diminished, while the intensity of the symmetric –(COO) elongation escalated [24].

3.3. Particle Size Analyzer. In order to determine the mean size diameter of the fabricated GO-Ag hybrid nanoparticle observed in Figure 4, the dynamic light scattering (DLS) method was applied. The DLS findings revealed that the synthesized nanocomposite has a mean particle size of 44 nm in precision and a particle size distribution of 30–80 nm.

3.4. Scanning Electron Microscope. Figure 5(a) illustrates the successful synthesis of an amorphous, worm-like structure of graphene oxide nanoparticles, forming silky wrinkled veils [26]. The image also highlights that the single-layer thickness of the GO nanosheet is greater than that of graphene due to the presence of covalently linked oxygen and displaced sp^3 hybridized carbon atoms, situated above and below the original graphene plane [7]. A small section of the image was analysed using ImageJ to determine the surface roughness of the GO nanoparticle, and the results confirmed that the GO nanosheet's surface was smooth, indicating that the formulation procedures and functional units were linked to the chemical process. On the other hand, the evenly distributed quasi-cubical Ag nanoparticles on the GO nano silk veil were found to have a rougher surface than the GO nanosheet (analysed in Image J), which confirms the firm decoration of Ag nanoparticles on the GO, as observed in Figure 5(b) (10 μm), Figure 5(c) (1 μm), and Figure 5(d) (300 nm).

3.5. EDS Analysis. The chemical composition analysis of GO-Ag hybrid nanofluids was conducted utilizing Energy Dispersive Spectroscopy (EDS), revealing weight percentages of carbon (C)—30.4%, oxygen (O)—39.8%, and silver (Ag)—29.8%, as summarized in Table 1. The presence of carbon, oxygen, and silver confirms the existence of graphene oxide and silver nanoparticles, respectively, in its combined form.

The elemental mappings depicted in Figure 6 illustrate the high purity and uniform distribution of Ag nanoparticles anchored over the GO nanosheets. The EDS analysis demonstrates the transmission of carbon and oxygen electrons from the K shell and Ag from the M shell due to their high ionization energies.

3.6. UV Vis Analysis. The UV spectral analysis results, depicted in Figure 7, confirm the successful formation of GO-Ag nanohybrids and are compared to the absorption band of GO nanoparticles. The nanofluids showed a pronounced absorption peak at wavelengths of 234 nm (GO) and 256 nm (GO-Ag), indicating the presence of GO nanoparticles [12]. The broad adsorption spectra at 400 nm (GO-Ag) correspond to the formation of Ag nanoparticles, which are not present in the GO spectrum. This is mainly due to the reflection of the Ag nanoparticle impinging on the surface of the GO nanosheet [12]. This Ag impingement results in a change in the formation of sp^2 polyaromatic carbon, causing a shift in the wavelength from 234 to 256 nm, signifying the partial reduction of GO during the synthesis of the GO-Ag nanohybrids. Moreover, it is associated with a significant reduction in the OH group spectral bands and changes in the asymmetrical and symmetrical spectral bands of GO-Ag, as revealed in the FTIR spectrum.

3.7. Thermal Conductivity. This section presents an investigation into the thermal conductivity of DW (0 wt.%) and GO-Ag hybrid nanofluid with different weight percentages (0.025 wt.%, 0.05 wt.%, 0.1 wt.%). Prior to evaluating the thermal conductivity (K) of the hybrid nanofluids, the K value of DW was measured and assessed using standard data (Incorpera, Dewitt, Bergman, and Lavine) [27], as depicted in Figure 8, which shows a good agreement between the measured and standard parameters.

The precise data was acquired by maintaining the GO-Ag nanofluid samples and the device in a constant-temperature bath for approximately fifteen minutes to achieve equilibrium. The mean of the observed values, with a correlation coefficient exceeding 0.99, was used to determine the sample's K value at a specific weight percentage.

The results indicate that the prepared hybrid nanofluids have a notable improvement in thermal conductivity with a temperature rise from 293 K to 333 K, as shown in Figure 9. This increase is primarily due to the Brownian motion of the dispersed GO-Ag nanoparticles in the base fluid, as the collision of the hybrid nanoparticles leads to the transfer of kinetic energy into thermal energy, resulting in the transfer of energy from the nanoparticles to the water molecules and an increase in the K value of the hybrid nanofluids.

Among the different concentrations and base fluids, the 0.1 wt.% hybrid nanofluid showed the most optimal results at both lower and higher temperatures. For example, at the temperature range of 293 K to 333 K, the thermal conductivity enhancement was about 6.69% to 15.29%, 11.04% to 22.63%, and 15.22% to 31.19% for 0.025 wt.%, 0.05 wt.%, and 0.1 wt.%, respectively, than the base fluid. This demonstrates that the K values increase linearly with temperature.

The thermal conductivity ratio (K_{nf}/K_{bf}) of GO-Ag was observed to be greater than one, signifying its superior performance and efficiency as a heat transfer fluid (Figure 10). Specifically, it was determined that the K_{nf}/K_{bf} increased within the ranges of 1.06–1.15, 1.11–1.22, and 1.15–1.31 for concentrations of 0.025 wt.%, 0.05 wt.%, and 0.1 wt.% over a temperature range of 293 K to 333 K, respectively, in comparison to the base fluid.

3.8. Viscosity. Viscosity (μ) plays a crucial role in influencing the heat flow in nanofluids. The increase in nanoparticle concentration in base fluids causes an increase in viscosity, which ultimately affects the heat transport capabilities. In this study, the viscosity of hybrid nanoparticles with three different weight percentages (0.025%, 0.05%, and 0.1%) was investigated using a Brookfield digital viscometer (LVDV-E, Brookfield, USA).

The viscosity of each sample was determined using spindle S61, which is specifically designed for low-viscosity fluids, while maintaining a consistent shear rate and spindle speed of 30 rpm. The viscosity of each sample was measured in five replicates.

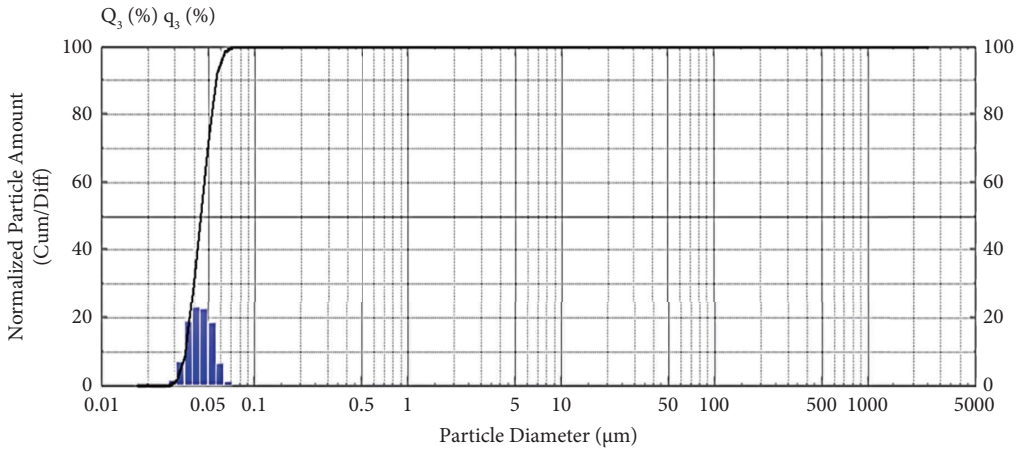

Figure 4: DLS result of GO-Ag hybrid nanoparticles.

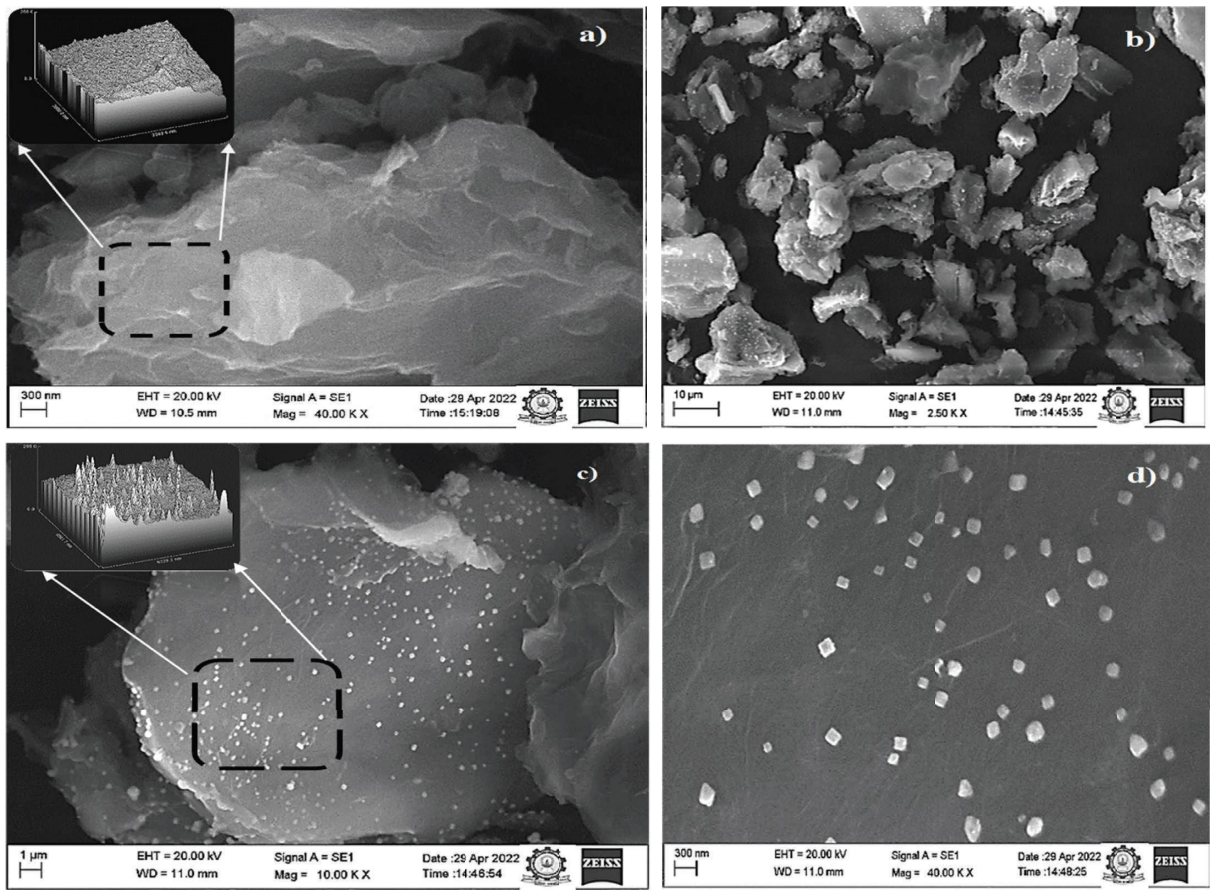

Figure 5: SEM image of (a) GO (300 nm), (b) GO-Ag (10 μm), (c) GO-Ag (1 μm), and (d) GO-Ag (300 nm).

Table 1: EDS analysis.

Elements	Wt. (%)	Atomic (%)	Error (%)	K ratio
C K	30.4	47.8	5.6	0.2067
O K	39.8	46.9	10.5	0.0584
Ag L	29.8	5.2	3.8	0.2475

The results shown in Figure 11 indicate that the viscosity of hybrid nanofluid decreases with increasing temperature. The viscosity of GO-Ag hybrid nanofluids does not vary significantly from that of the base fluid, and the difference in viscosity between GO-Ag nanofluids and the base fluid decreases as the temperature increases. At 293 K, the viscosity of 0.1 wt.% was higher than that of other nanofluid concentrations. However, as the temperature increased, the viscosity of 0.1 wt.% approached that of the base fluid viscosity. The findings suggest that the μ values increase exponentially with an increasing proportion of GO-Ag nanoparticles. However, as the temperature rises with higher concentrations of nanoparticles, viscosity decreases at

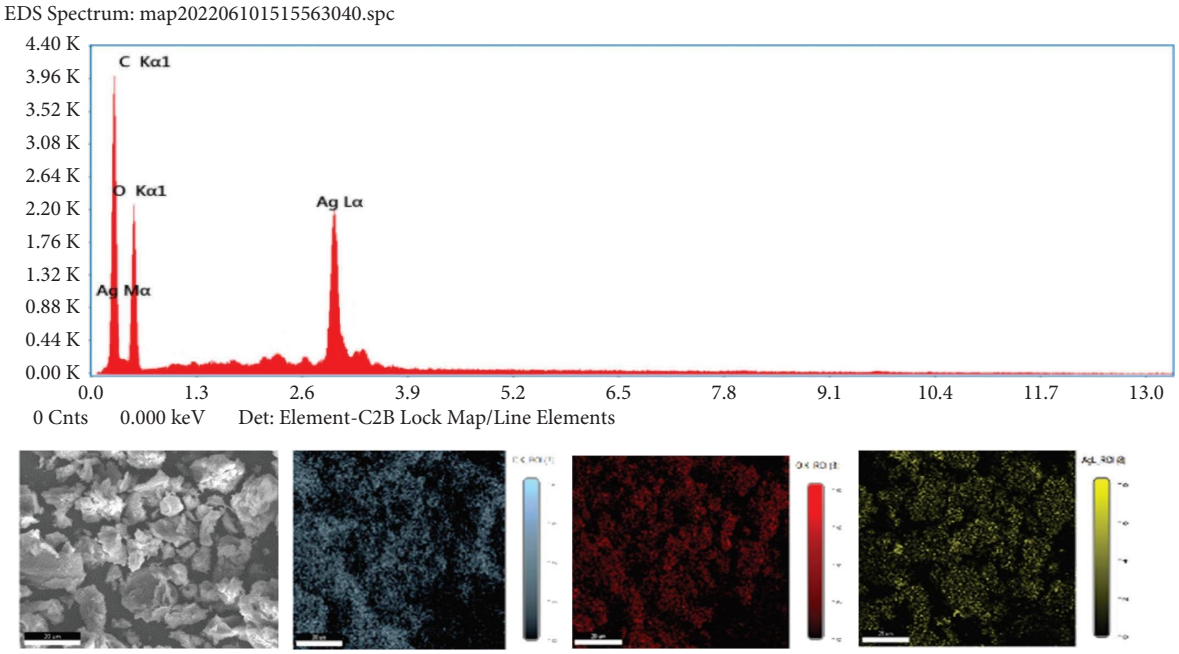

Figure 6: EDS analysis of GO-Ag nanoparticles and elemental mapping of SEM image, C, O, and Ag.

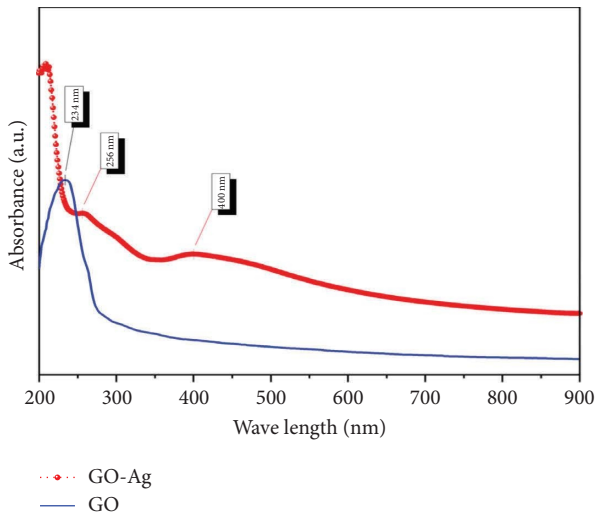

Figure 7: UV-absorbance spectrum of GO and GO-Ag hybrid nanoparticles.

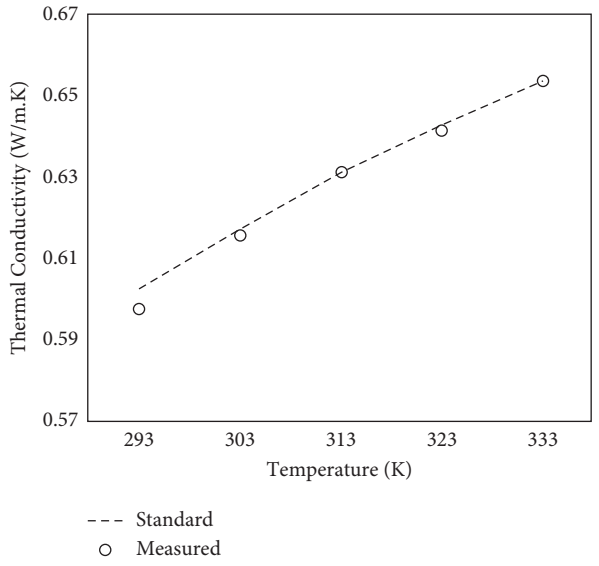

Figure 8: Measured and standard values of DW.

a faster pace. This happens because an increase in temperature reduces the density of the fluid, limiting the shearing force between fluid interfaces.

4. Validation of Results

4.1. Comparison between Experimental Results of (K_{nf}/K_{bf}) and Standard Correlated Models. In order to relate the experimental results (K_{nf}/K_{bf}) to the appropriate correlated standard models, some well-known prominent thermal conductivity models from the past and present were used in this study. Like the Maxwell model [28] in (2), it is the most popular, conventional, and used by many researchers to correlate their experimental findings, where K_{nf} is the thermal conductivity of the nanofluid, K_{bf} is the thermal conductivity of the base fluid, and K_p is the nanoparticle thermal conductivity coefficient.

$$\frac{K_{nf}}{K_{bf}} = \frac{\left(2K_{bf} + K_p + 2\varphi\left(K_p - K_{bf}\right)\right)}{2K_{bf} + K_p - \varphi\left(K_p - K_{bf}\right)}. \tag{2}$$

Furthermore, Timofeeva et al. [29], in equation (3), analysed several nanoparticles and offered a concentration-based thermal conductivity ratio relationship.

$$\frac{K_{nf}}{K_{bf}} = (1 + 3\varphi). \tag{3}$$

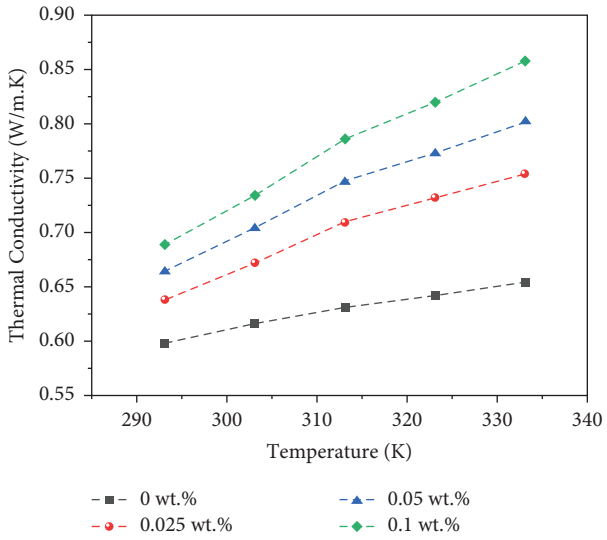

Figure 9: Results on K value of GO-Ag nanofluids.

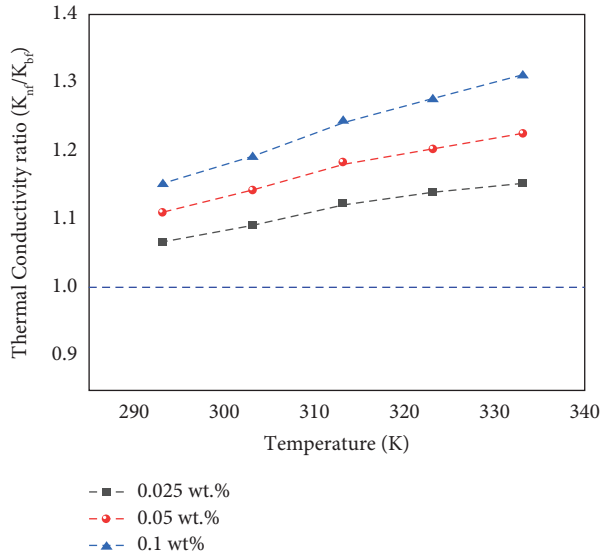

Figure 10: Thermal conductivity ratio (K_{nf}/K_{bf}) of GO-Ag nanofluids.

Later, Lu and Lin [30], in equation (4), similar to Timofeeva et al., postulated a relationship based on nanoparticle concentration.

$$\frac{K_{nf}}{K_{bf}} = \left(1 + 2.25\varphi + 2.27\varphi^2\right). \quad (4)$$

While experimenting with the thermophysical characteristics of graphene oxide and alumina nanoparticles, Taherialekouhi et al. [18], in equation (5), suggested a model between both the concentration and temperature of nanoparticles as dependent elements.

$$\frac{K_{nf}}{K_{bf}} = \left(0.031 * \left(T^{1.185}\right) * \left(\varphi^{0.863}\right) + 1.006\right). \quad (5)$$

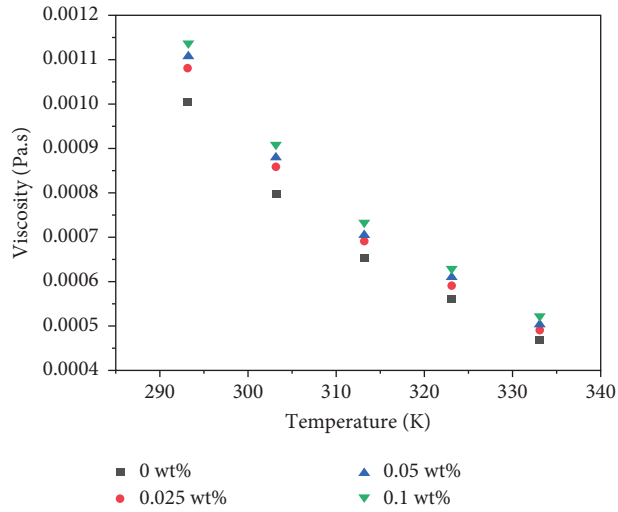

Figure 11: The viscosity of GO-Ag nanofluid.

The empirical thermal conductivity ratio of the GO-Ag nanofluid was compared to various standard models, and the results were presented in Figures 12(a)–12(e). It was observed that the empirical K_{nf}/K_{bf} of the nanofluid performed significantly better than the standard models. For instance, at 333 K, the experimental K_{nf}/K_{bf} of GO-Ag showed a remarkable increase of 12.67% compared to the Taherialekouhi et al. model. Hence, the empirical K-ratio results were found to deviate from the standard relations mentioned earlier. However, to investigate the thermal conductivity of GO-Ag nanofluid, a suitable mathematical model was proposed using the response surface methodology (RSM) approach. We meticulously analysed the experimental thermal conductivity ratio and precisely predicted a mathematical model that fits the experimental data.

4.2. RSM Regression Model. The Response Surface Methodology (RSM) approach was employed to establish a linear correlation in this study. Response surface regression analysis is a well-known technique in design of experiments (DOE) applications [20, 31]. The input data was examined with respect to the experimentally measured results to determine the final output. The primary objective was to create a statistical and mathematical model based on empirical K ratio values of GO-Ag nanofluid. The accuracy and reliability of the created regression model were evaluated using the analysis of variance (ANOVA) approach, as presented in Table 2. A correlation between the predicted and experimental results can only be achieved when the R^2 value is close to one. In this study, the regression analysis of the experimental results produced an R^2 value of 0.99, indicating a better correlation between predicted and empirical values. The quadratic regression analysis was preferred over other analyses such as 2FI, linear, and cubic, as it resulted in a very low p value of 0.0001 and a higher Fisher test value (F-value). The p value should be less than 0.05 to achieve better optimization [20]. The predicted equation for the K

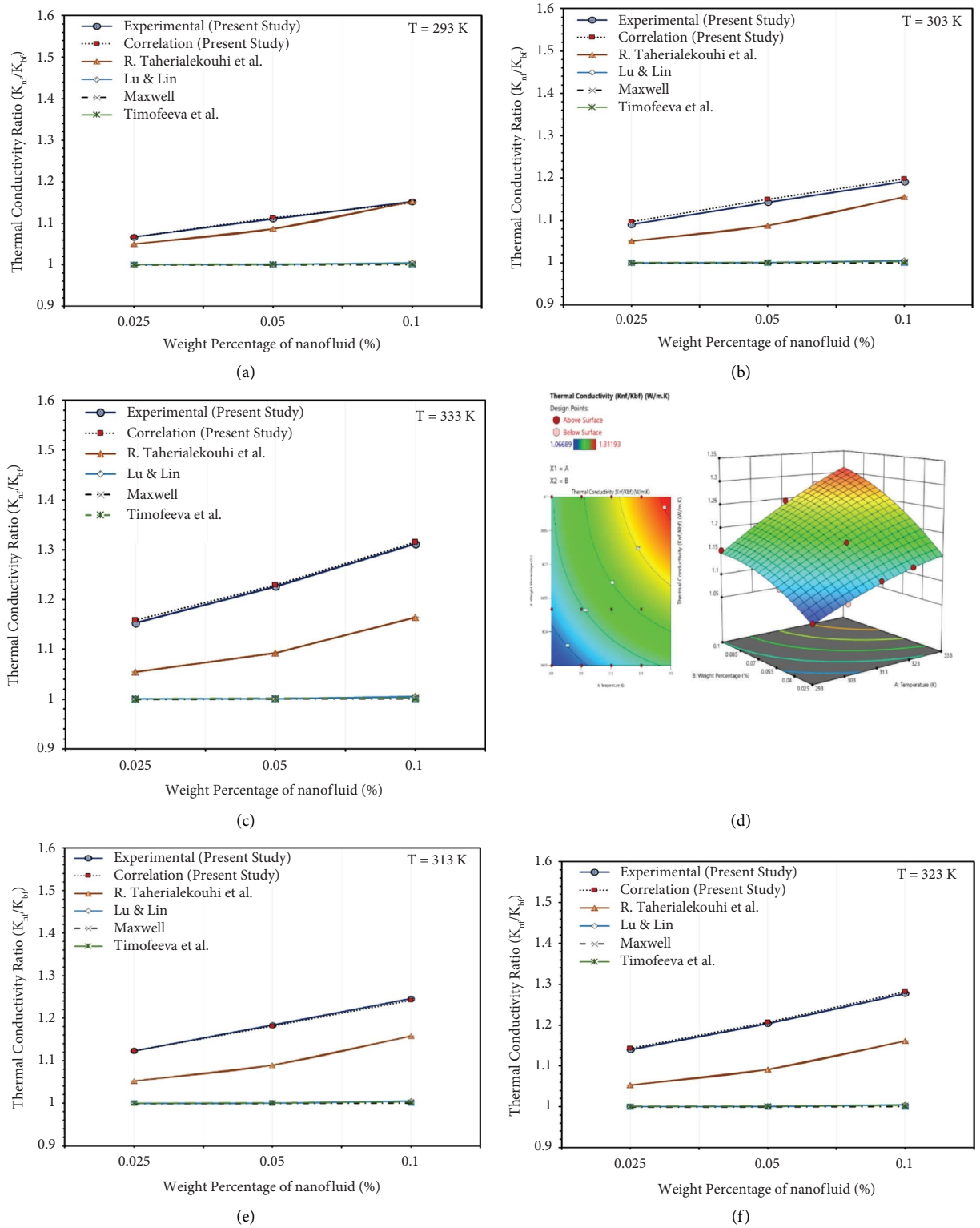

Figure 12: (a–e) Comparison of weight percentage of nanofluids vs thermal conductivity ratio at different temperatures ranging from 293 K–333 K, and (f) contour and three-dimensional diagram of the proposed correlation.

ratio of the GO-Ag nanofluid is provided by equation (6), with temperature (T in K) and weight percentage (φ) as constraint factors at low and higher concentrations ($0.025\ \text{wt.\%} < \varphi < 0.1\ \text{wt.\%}$) of GO-Ag hybrid nanofluids. The nanoparticle concentration factor (φ) in the proposed model was found to be the most significant and preferable factor compared to temperature based on the variance analysis results.

Table 2: ANOVA-type III-partial sum of squares.

Source	Sum of squares	*Df*	Mean square	*F*-value	*p*-value	
Model-K_{nf}/K_{bf}	0.0664	5	0.0133	452.85	<0.0001	Significant
A-Temperature	0.0301	1	0.0301	1027.30	<0.0001	
B-Weight percentage	0.0356	1	0.0356	1212.21	<0.0001	
AB	0.0018	1	0.0018	62.89	<0.0001	
A^2	0.0003	1	0.0003	8.96	0.0151	
B^2	0.0011	1	0.0011	38.58	0.0002	
Residual	0.0003	9	0			
Cor total	0.0667	14				

$$\frac{K_{nf}}{K_{bf}} = 0.017294T - 4.40638\varphi + 0.025153T\varphi - 0.000025T^2 - 15.01048\varphi^2 - 1.91857. \quad (6)$$

The regression model proposed using RSM analysis accurately fits the experimental data, with most of the predicted points being close to the experimental values shown in Figures 12(a)–12(e).

The contour and three-dimensional diagrams of the proposed model are presented in Figure 12(f). It was observed that the K_{nf}/K_{bf} improved with an increase in both T and φ of nanoparticles. Figure 13 compares the empirical and predicted results of K_{nf}/K_{bf}, showing the maximum percentage deviation between empirical and predicted to be ±1.2%. This deviation indicates an acceptable mathematical correlation with the experimental results. Table 3 shows the comparison between the results of the actual and predicted thermal conductivity ratios of GO-Ag hybrid nanofluids with residual errors, leverage, and externally studentized residuals.

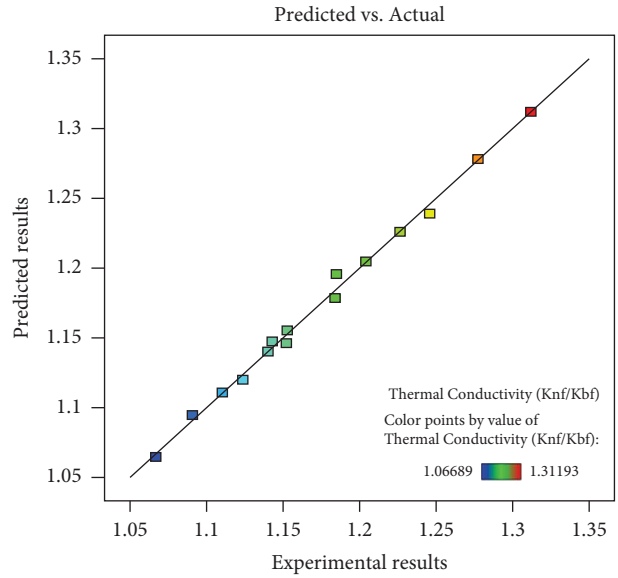

Figure 13: Predicted results vs experimental results.

5. Processes Governing Thermal Conductivity Augmentation in GO-Ag Nanofluid

The impact of several key processes enhanced the K value of GO-Ag hybrid nanofluids. Following are a few contributing factors that impact the improvement of thermal conductivity.

(1) Brownian motion [15, 32]: As the temperature of the hybrid nanofluids increased, the dispersed GO-Ag hybrid nanoparticles began to move randomly due to the excess heat. This resulted in relative lateral motion and collisions between the particles, converting kinetic energy to thermal energy and dissipating it to the base fluid's molecules. This prolonged contact between particles and molecules promoted microconvectional heat transport, enhancing nanoscale conduction and convection heat transfer.

(2) Clustering of nanoparticles [33, 34]: The surface area of GO and Ag nanoparticles is increased due to clustering, as observed in SEM images of Ag nanoparticles clustered on the surface of GO nanosheets. These clusters improve interaction with the fluid layers, enhancing microconvective heat transfer and thermal conductivity. The liquid layers adjacent to the enhanced surface behave like solid surfaces at the solid-liquid interface, improving heat transfer from the nanoparticle to its next liquid layer.

(3) Electron-phonon collision: A relatively high thermal conductivity performance factor was observed at higher temperatures, possibly due to the aforementioned factors. Electron-hole pair excitation and electron-electron collisions may occur in dispersed hybrid nanoparticles due to thermal effects. The presence of external energy results in electron lattice collisions, coupling low-level energy electrons to phonons, and increasing the temperature of metal lattices. Heat produced in the metal lattice dissipates into the surrounding fluid molecules through phonon-phonon scattering [35]. This phenomenon causes the heat to dissipate from the energized nanoparticles into the base fluid, contributing to the increase in thermal conductivity.

(4) Other factors, including surface chemical effects, atomic force, crystalline nature, and nanoscale rotation of nanoparticles due to temperature increase, also contribute to the development of the K value of the hybrid system.

Table 3: Comparison of actual and predicted thermal conductivity ratios.

Wt. (%)	Temperature (K)	Actual *K*-ratio	Predicted *K*-ratio	Percentage of deviation (%)	Residual	Leverage	Externally studentized residuals
0.025	293	1.0669	1.0674	0.0519	0.002	0.581	0.54
	303	1.0909	1.0977	0.6194	−0.004	0.295	−0.867
	313	1.1236	1.1228	−0.0718	0.0037	0.295	0.792
	323	1.1402	1.1430	0.2451	0.0003	0.295	0.061
	333	1.1529	1.1581	0.4494	−0.0019	0.581	−0.531
0.05	293	1.1104	1.1135	0.2819	−0.0006	0.438	−0.127
	303	1.1429	1.1498	0.6116	−0.0044	0.26	−0.924
	313	1.1838	1.1814	−0.2059	0.0053	0.295	1.198
	323	1.2041	1.2078	0.3140	−0.0007	0.26	−0.145
	333	1.2263	1.2293	0.2467	0.0003	0.438	0.066
0.1	293	1.1522	1.1666	1.2497	0.0055	0.667	2.021
	303	1.1851	1.1982	1.1121	−0.0105	0.317	−3.522
	313	1.2456	1.2424	−0.2637	0.0062	0.295	1.439
	323	1.2773	1.2814	0.3253	−0.001	0.317	−0.212
	333	1.3119	1.3153	0.2574	−0.0002	0.667	−0.049

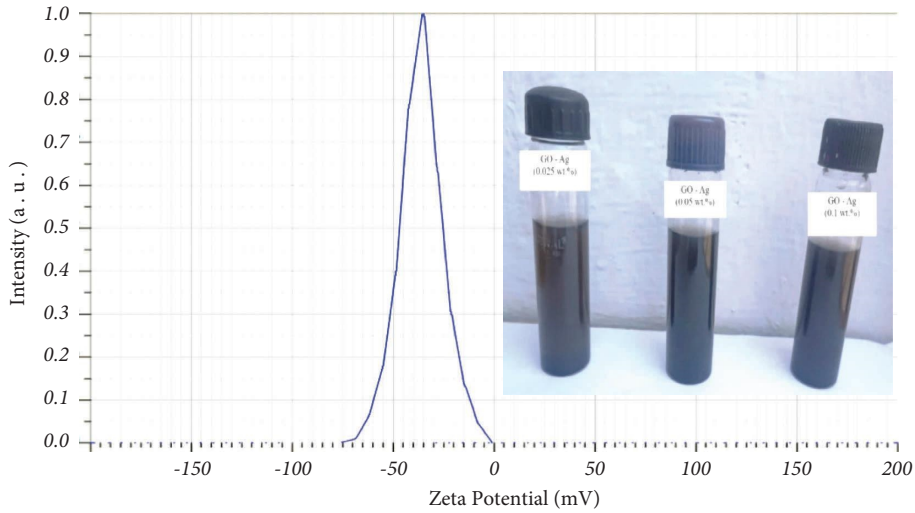

Figure 14: Zeta potential analysis and pictorial view of prepared samples.

6. Stability

The dissemination of hybrid nanoparticles in the base fluid was confirmed by conducting zeta potential [34] and UV-visible spectra [15] analyses using nanofluids at all concentrations of GO-Ag (0.025 wt.%, 0.05 wt.%, and 0.1 wt.%). The electrokinetic potential (zeta potential) value was measured to indicate the repulsive force and stability of the nanoparticles in the base fluid. The greater the values of the zeta potential (either positive or negative), the greater the stability of the nanofluids.

Nanofluids with a value greater than ±30 mV were considered to possess higher repulsive forces between particle suspensions, resulting in less agglomeration and good stability [34]. The zeta potential result of the GO-Ag hybrid nanofluid sample, as shown in Figure 14, had a mean value of −35.6 mV, indicating that the nanofluid was highly stable with a considerable negative repellent potential.

Furthermore, the UV absorbance of the silver nanoparticles at $\lambda = 400$ nm in GO-Ag hybrid nanofluids was analysed in Figure 15. The observed results showed hardly any changes in wavelength or absorbance value after 25 days of measurements in the UV-visible spectrometer, demonstrating the high stability of the hybrid nanofluids. This stability might be due to the functional group on the interface of the GO nanoparticles, which anchored the strong bond with the Ag nanoparticles, and the influence of reducing and stabilizing agents on the Ag nanosurface decreased the agglomeration of nanoparticles to settle down and in reaction with water molecules. Therefore, it is presumed that the prepared hybrid nanofluids are stable in all applications.

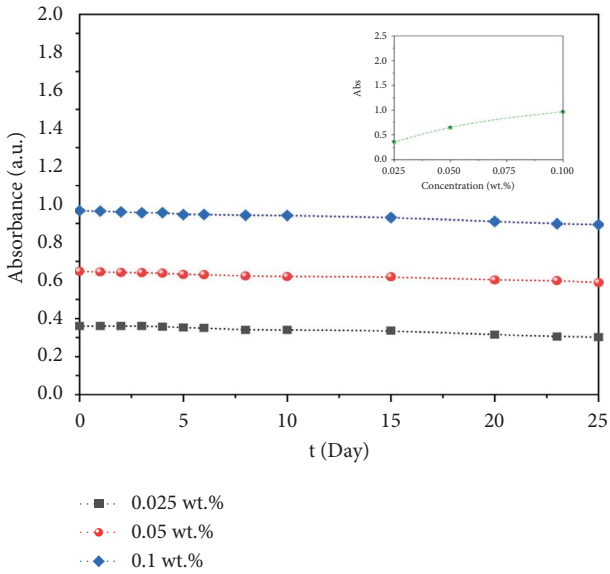

Figure 15: UV absorbance spectrum of GO-Ag nanofluids at $\lambda = 400$ nm.

7. Conclusion

The low-cost chemical reduction technique was utilized to synthesize the GO-Ag hybrid nanoparticles. A detailed experimental investigation was conducted on the preparation, characterization, and thermophysical properties of the GO-Ag hybrid nanofluids at different weight percentages. The following findings were established:

(1) The particle size analyzer, XRD, FTIR, UV, SEM, and EDX analyses demonstrated that the hybrid structure comprised significant molecular linkages of all elements (GO and Ag).

(2) The K and μ values of the hybrid nanofluids were found to be in agreement and increased with increasing concentrations of the nanoparticles.

(3) At 333 K temperature in 0.1 wt.%, the GO-Ag nanofluid exhibited the highest thermal conductivity enhancement of 31.19% compared to the base fluid.

(4) The K ratio of GO-Ag hybrid nanofluids was evaluated by comparing it to standard models. A mathematical relationship was derived using RSM methodology based on the empirical values of the thermal conductivity of GO-Ag hybrid nanofluids as a function of temperature and weight percentage. Compared to other standard equations discussed, the derived equation showed a better correlation with the empirical results.

(5) Zeta potential and UV visible spectrum analyses confirmed the stability of the nanofluids. Due to their improved thermophysical properties, GO-Ag nanofluids could be an excellent choice for heat transport fluids in applications such as solar-thermal and heat exchanging equipment.

Data Availability

The data used to support the findings of this study are available from the corresponding author upon request.

Conflicts of Interest

The authors declare that there are no conflicts of interest.

Authors' Contributions

M. Armstrong conceptualised the study, was responsible for nanoparticles selection, synthesis, characterization, and experimentation, and was responsible for Software, data curation, and manuscript preparation. M. Sivasubramanian performed supervision, experimental testing, and manuscript verification. N. Selvapalam and R. Pavitra were responsible for cosupervision and guidance in nanoparticle preparation. P. Rajesh KAnna and Haiter Lenin cosupervised the study and verified the manuscript.

Acknowledgments

The authors expressed their gratitude to the Department of Mechanical Engineering and the International Research Centre at the Kalasalingam Academy of Research and Education for allowing them to use all the laboratories.

References

[1] M. Asim and F. R. Siddiqui, "Hybrid nanofluids—next-generation fluids for spray-cooling-based thermal management of high-heat-flux devices," *Nanomaterials*, vol. 12, no. 3, p. 507, 2022.

[2] A. T. Smith, A. M. LaChance, S. Zeng, B. Liu, and L. Sun, "Synthesis, properties, and applications of graphene oxide/reduced graphene oxide and their nanocomposites," *Nano Materials Science*, vol. 1, pp. 31–47, 2019.

[3] C. Rajaganapathy, D. Vasudevan, and N. Selvakumar, "Investigation on Tribological and mechanical behaviour of AA6082- graphene based composites with Ti particles," *Materials Research Express*, vol. 7, Article ID 076514, 2020.

[4] K. K. Jha, M. Armstrong, S. S. Kumar, M. V. Kumar, and G. S. S. Charan, "A recent examination on the performance of heat pipes in nanofluids in enhancing the thermodynamic properties," *Materials Today: Proceedings*, vol. 60, pp. 1920–1926, 2022.

[5] A. S. Manirathnam, M. Dhanush Manikandan, R. Hari Prakash, B. Kamesh Kumar, and M. Deepan Amarnath, "Experimental analysis on solar water heater integrated with Nano composite phase change material (SCi and CuO)," *Materials Today: Proceedings*, vol. 37, pp. 232–240, 2021.

[6] P. Majumder and R. Gangopadhyay, "Evolution of graphene oxide (go)-based nanohybrid materials with diverse compositions: an overview," *RSC Advances*, vol. 12, pp. 5686–5719, 2022.

[7] Z. Hajjar, A. M. Rashidi, and A. Ghozatloo, "Enhanced thermal conductivities of graphene oxide nanofluids," *International Communications in Heat and Mass Transfer*, vol. 57, pp. 128–131, 2014.

[8] X. Mei, X. Sha, D. Jing, and L. Ma, "Thermal conductivity and rheology of graphene oxide nanofluids and a modified

predication model," *Applied Sciences*, vol. 12, no. 7, p. 3567, 2022.

[9] W. Raza and S. B. Krupanidhi, "Retraction of: Engineering defects in graphene oxide for selective ammonia and enzyme-free glucose sensing and excellent catalytic performance for para-nitrophenol reduction," *ACS Applied Materials and Interfaces*, vol. 11, no. 2, p. 2560, 2019.

[10] M. C. Mbambo, M. J. Madito, T. Khamliche, C. B. Mtshali, Z. M. Khumalo, and I. G. Madiba, "Thermal conductivity enhancement in gold decorated graphene nanosheets in ethylene glycol based nanofluid," *Scientific Reports*, vol. 10, no. 1, Article ID 14730, 2020.

[11] M. Armstrong, M. Sivasubramanian, and N. Selvapalam, "A review on the enhancement of heat exchanging process using TiO_2 Nanofluids," *Lecture Notes in Mechanical Engineering*, Springer, Singapore, 2020.

[12] M. Cobos, I. De-La-pinta, G. Quindós, M. D. Fernández, and M. J. Fernández, "Graphene oxide–silver nanoparticle nanohybrids: synthesis, characterization, and antimicrobial properties," *Nanomaterials*, vol. 10, 2020.

[13] K. Elsaid, M. A. Abdelkareem, H. M. Maghrabie et al., "Thermophysical properties of graphene-based nanofluids," *International Journal of Thermofluids*, vol. 10, Article ID 100073, 2021.

[14] M. Armstrong, M. Sivasubramanian, N. Selva Palam, M. Adam Khan, and C. Rajaganapathy, "A recent examination on the nano coating techniques in heat transfer applications," *Materials Today: Proceedings*, vol. 46, pp. 7942–7947, 2021.

[15] D. Li, Y. Wang, M. Guo, M. Song, and Y. Ren, "Preparation and thermophysical properties of graphene oxide-silver hybrid nanofluids," *Bulletin of Materials Science*, vol. 43, no. 1, p. 147, 2020.

[16] G. Huminic, A. Vărdaru, A. Huminic, C. Fleacă, F. Dumitrache, and I. Morjan, "Water-based graphene oxide–silicon hybrid nanofluids—experimental and theoretical approach," *International Journal of Molecular Sciences*, vol. 23, no. 6, p. 3056, 2022.

[17] J. Singh, R. Kumar, M. Gupta, and H. Kumar, "Thermal conductivity analysis of GO-CuO/DW hybrid nanofluid," *Materials Today: Proceedings*, vol. 28, pp. 1714–1718, 2020.

[18] R. Taherialekouhi, S. Rasouli, and A. Khosravi, "An experimental study on stability and thermal conductivity of water-graphene oxide/aluminum oxide nanoparticles as a cooling hybrid nanofluid," *International Journal of Heat and Mass Transfer*, vol. 145, Article ID 118751, 2019.

[19] N. M. El-Shafai, R. Ji, M. Abdelfatah et al., "Investigation of a novel (GO@CuO.γ-Al2O3) hybrid nanocomposite for solar energy applications," *Journal of Alloys and Compounds*, vol. 856, 2021.

[20] R. Vidhya, T. Balakrishnan, and B. S. Kumar, "Experimental and theoretical investigation of heat transfer characteristics of cylindrical heat pipe using Al2O3–SiO2/W-EG hybrid nanofluids by RSM modeling approach," *Journal of Engineering and Applied Science*, vol. 68, no. 1, p. 32, 2021.

[21] M. Armstrong, M. Sivasubramanian, N. Selvapalam, and C. Rajaganapathy, "Revving up heat transfer performance of double pipe heat exchanger using diverse molar Ag-GO hybrid nanofluids: an Empirical and Numerical study using Central Composite Design," *Journal of Enhanced Heat Transfer*, vol. 30, 2023.

[22] M. Behrouz, S. Dinarvand, M. E. Yazdi, H. Tamim, I. Pop, and A. J. Chamkha, "Mass-based hybridity model for thermo-micropolar binary nanofluid flow: first derivation of angular momentum equation," *Chinese Journal of Physics*, vol. 83, pp. 165–184, 2023.

[23] W. S. Hummers and R. E. Offeman, "Preparation of graphitic oxide," *Journal of the American Chemical Society*, vol. 80, no. 6, p. 1339, 1958.

[24] K. S. Hui, K. N. Hui, D. A. Dinh et al., "Green synthesis of dimension-controlled silver nanoparticle-graphene oxide with in situ ultrasonication," *Acta Materialia*, vol. 64, pp. 326–332, 2014.

[25] Y. Qin, X. Ji, J. Jing, H. Liu, H. Wu, and W. Yang, "Size control over spherical silver nanoparticles by ascorbic acid reduction," *Colloids and Surfaces A: Physicochemical and Engineering Aspects*, vol. 372, no. 1-3, pp. 172–176, 2010.

[26] M. Mehrali, E. Sadeghinezhad, M. A. Rosen et al., "Experimental investigation of thermophysical properties, entropy generation and convective heat transfer for a nitrogen-doped graphene nanofluid in a laminar flow regime," *Advanced Powder Technology*, vol. 27, no. 2, pp. 717–727, 2016.

[27] P. Frank Incorpera, P. David Dewitt, L. Theodeore Bergman, and S. Adrienne Lavine, *Fundamentals of Heat and Mass Transfer*, John Wiley & Sons, River Street, HB, USA, 6th edition, 2007.

[28] C. M. James, *A Treaties on Electricity and Magnetism*, Clarendon Press, Oxford, England, 1873.

[29] E. V. Timofeeva, A. N. Gavrilov, J. M. McCloskey, Y. V. Tolmachev, S. Sprunt, and L. M. Lopatina, "Thermal conductivity and particle agglomeration in alumina nanofluids: experiment and theory," *Physical Review*, vol. 76, no. 6, Article ID 061203, 2007.

[30] S. Y. Lu and H. C. Lin, "Effective conductivity of composites containing aligned spheroidal inclusions of finite conductivity," *Journal of Applied Physics*, vol. 79, pp. 6761–6769, 1996.

[31] P. A. Karthick, S. R. Kumar, P. Prathap, K. Ragul, and K. S. Raghul, "Optimization of reaming parameters to improve surface roughness of En1A leaded material with the approach of particle swarm optimization," *Materials Today Proceedings*, vol. 37, pp. 1003–1008, 2020.

[32] M. F. Nabil, W. H. Azmi, K. A. Hamid, N. N. M. Zawawi, G. Priyandoko, and R. Mamat, "Thermo-physical properties of hybrid nanofluids and hybrid nanolubricants: a comprehensive review on performance," *International Communications in Heat and Mass Transfer*, vol. 83, pp. 30–39, 2017.

[33] I. Gonçalves, R. Souza, G. Coutinho et al., "Thermal conductivity of nanofluids: a review on prediction models, controversies and challenges," *Applied Sciences*, vol. 11, no. 6, p. 2525, 2021.

[34] M. Armstrong, S. Mahadevan, N. Selvapalam, C. Santulli, S. Palanisamy, and C. Fragassa, "Augmenting the double pipe heat exchanger efficiency using varied molar Ag ornamented graphene oxide (GO) nanoparticles aqueous hybrid nanofluids," *Frontiers in Materials*, vol. 10, Article ID 1240606, 2023.

[35] D. Mateo, J. L. Cerrillo, S. Durini, and J. Gascon, "Fundamentals and applications of photo-thermal catalysis," *Chem Soc Rev.*, vol. 50, pp. 2173–2210, 2021.